Fracture and fatigue performance of textile commingled yarn composites

M. D. GILCHRIST
Department of Mechanical Engineering, University College Dublin, Belfield, Dublin 4, IRELAND

N. SVENSSON
Pelmatic Consulting Engineers, F O Petersons gata 28, S-42131, Västra Frölunda, SWEDEN

R. SHISHOO
Swedish Institute for Fibre and Polymer Research, P.O.Box 104, S-43122 Mölndal, SWEDEN

The response to mechanical loads of commingled warp knitted and woven glass fibre reinforced polyethylene terephthalate (GF/PET) laminates has been characterised. The mechanical properties of the two materials were determined under tension, in-plane shear and flexure. The flexural fatigue properties were determined for the woven laminates by means of three point bending tests with a loading ratio of R=0.1 at stress levels of 50-90% of the ultimate static strength. The Mode I, Mode II and mixed mode (Mode I:II ratios 4:1, 1:1 and 1:4) interlaminar fracture toughnesses of the laminates were determined by means of the double cantilever beam (DCB) and mixed mode bending (MMB) tests respectively. The main fractographic features, as determined by an scanning electron microscopy (SEM) examination, of the Mode I dominated failures were a brittle matrix failure and larger amounts of fibre pull-out. As the Mode II loading component increased, the amount of fibre pull-out was reduced and the features of the matrix appeared to be more sheared. Cusps were found on the fracture surfaces of specimens tested in pure Mode II and mixed mode I:II=1:4. Cusps are normally not found in thermoplastic matrix composites.

Keywords: commingled yarn, fatigue, fractography

Introduction

The interest in using textile thermoplastic composite materials has increased substantially within the past decade. This is due to a number of reasons [1-5]: (i) it is much easier to recycle thermoplastic matrix composites than those based on thermoset resins, (ii) the shelf life of a thermoplastic matrix prepreg is almost unlimited and there are no requirements for storage at sub-zero temperatures, (iii) there is large potential for fast automated manufacturing, compare compression moulding and diaphragm moulding of glass mat thermoplastic (GMT) materials, (iv) thermoplastic composites may be post-shaped and welded, (v) a thermoplastic matrix has a longer elongation at fracture and a higher resistance to crack propagation than ordinary thermoset matrices and (vi) textile processes, such as weaving, braiding and knitting, enable faster fabrication and tailoring of the fibre architecture of preforms than currently offered by conventional and prepreg techniques.

Commingled yarns, i.e. yarns in which the reinforcing fibres are intimately mixed with spun thermoplastic matrix fibres, are a novel form of intermediate materials suitable for manufacturing load carrying thermoplastic composites. As the yarns are flexible, they can be used in any textile process. Consequently drapable and highly conformable fabrics and structures may be produced. A wide variety of fibre/matrix combinations are available in commingled form [6]. Production cycle times range from below one minute to several hours depending on the matrix material as well as on the required pressure and processing temperature. Process control is crucial as overheating degrades the matrix material and reduces the final composite properties. A pressure of 0.3-1.5MPa is required for good consolidation in a reasonable time and the cooling should preferably be rapid to prevent the formation and growth of large spherulites in semi-crystalline polymer matrices. Pressure applied during cooling hinders deconsolidation which deteriorates the mechanical properties of the composite.

The present work describes the mechanical response under tension, in-plane shear and flexure of thermoplastic laminates manufactured from warp knitted and woven fabrics. The flexural

fatigue behaviour was characterised together with the resistance to interlaminar crack propagation in Mode I, Mode II and mixed modes (I:II) 4:1, 1:1 and 1:4. A scanning electron microscopy (SEM) analysis was conducted to elucidate the fracture processes and the laminate quality.

Experimental procedures

The constituents of the commingled yarn used were glass fibres and PET fibres. The glass fibre volume fraction in the yarns was 48% and the yarns were produced by means of air-jet texturising. The laminates were manufactured from woven and warp knitted fabrics. The woven fabric was tailored with the main fraction (5/6) of the fibres being aligned in the warp direction. The warp knitted fabric was unidirectional and the commingled yarns were held together by a thin PET yarn, Fig. 1.

The formability, i.e. bending and shear properties, and the compression behaviour of the two fabrics were examined [7] by means of the Kawabata Evaluation System (KES), which is an established method for the characterisation of mechanical and surface properties of fabrics and non-wovens.

The fabrics were cut and stacked to produce unidirectional and cross-ply laminates. 20 layers were used for the warp knitted fabric and 12 layers for the woven fabric. Steel guide bars were used to obtain a uniform laminate thickness. The consolidation pressure was provided by compacting the fabric stacks from the uncompressed thickness of about 12mm to the target thickness of 3mm. The warp knitted fabrics were more difficult to compress and the warp knitted cross ply laminates consequently resulted in a thickness of 4mm. A Nylon6 film with a thickness of 50μm and coated with release agent was used to induce starter cracks in the laminates that were subsequently used for fracture toughness testing.

The laminates were compression moulded in a hydraulic press between steel platens. The mould was heated to 210ºC within 20min and the consolidation time was also 20min. The cooling

rate was 21ºC/min. Pressure was applied during heating as well as during cooling. The glass fibre volume fraction for the laminates was determined by matrix burn-off and was determined to be 48.1%. The quality of the laminates was examined by observing polished cross-sections in an optical microscope. The T_g of the PET matrix was determined by means of dynamical mechanical thermal analysis (DMTA) to be 75.8°C. A number of the woven laminates were annealed for three hours at 110ºC to investigate if any differences in fracture properties could be observed as a result of the different thermal histories and hence different microstructures. This is discussed further in the following section.

The warp and weft direction tensile properties of the two different kinds of laminates were determined in accordance with ASTM D3039. The in-plane shear behaviour was determined following ASTM D3518. The static flexural properties of the laminates were determined in the warp and weft directions using a three point bend test, ASTM D790M, with a span to thickness ratio of 16:1.

For the fatigue tests, three point bending with a span to thickness ratio of 32:1 was used. The woven material was characterised in fatigue. A loading ratio of R=0.1 (The loading ratio defines the ratio of minimum to maximum load during a complete fatigue cycle.) was used at five different load levels, i.e. 50%, 60%, 70%, 80% and 90% of the static flexure failure load. At least three specimens were tested at each load level.

The fracture mechanics specimens were cut using a band saw and the edges of the specimens were polished and coated with typewriter correction fluid and the crack tip was marked on the edges of the specimens. The specimen dimensions were in accordance with the double cantilever beam (DCB) test, ASTM D5528. The Mode I tests were carried out by means of the DCB test. For pure Mode II tests and mixed modes (Mode I to Mode II loading ratio) 4:1, 1:1 and 1:4 tests the modified mixed mode bending (MMB) geometry [8-10] was used. An investigation of the fracture surfaces was carried out by means of a JEOL scanning electron microscope and the fracture surfaces was sputter coated with gold prior to the SEM examination.

Results and discussion

The two fibre architectures that had been used made the fabrics very drapable, especially in the weft direction. Consequently they were difficult to handle and align and variations in fibre angles between the plies in the laminates were inevitable. Due to the high draw ratio required for spinning the matrix fibres these are highly aligned and additional fibre misalignment in the composites may have been caused by contraction of these matrix fibres on heating. The crimp (i.e. the undulation of the warp and weft fibres) in the woven laminates, was responsible for the large resin pockets in the material, especially in the cross-over areas between the warp and weft bundles. The fibre distribution was good outside the resin pockets. The reinforcing fibres in the warp knitted fabrics were non-crimped and there were fewer and smaller resin pockets than in the woven laminates. Cracks were occasionally seen in and between the fibre bundle in both types of laminates. Very few voids were seen in the matrix. Similar observation in woven commingled GF/PET laminates have been made by Ye and Friedrich [11] who also reported large amounts of small voids in the resin rich regions between the warp and weft bundles in woven GF/PET laminates and these were caused by shrinkage upon crystallisation. Angles between fibre bundles promoted the formation of voids. Shonaike *et al.* [12] examined commingled GF/PET composites and noted that the crystallinity of the matrix was not affected by different holding times during compression moulding. At short consolidation times many voids were whereas at consolidation times >5min the impregnation was complete without any voids. Neither the melting temperature nor the crystallisation temperature of the composite were affected by the holding time during consolidation. The fibre/matrix adhesion in the present material system was poor as can be seen from the very clean glass fibres in Fig. 2 which is a micrograph from a woven mixed mode 1:1 fracture specimen.

Tension and in-plane shear

Neither matrix cracking nor fibre fracture was observed prior to failure during warp direction tensile tests. Failure of these test specimens occurred very suddenly although the specimens did not shatter dramatically in the fashion of unidirectional prepreg laminates. A limited amount of longitudinal splitting occurred at failure in the warp knitted laminates. A small stiffening was apparent for both materials as the load increased and this was attributed to reorientation of the misaligned glass fibres during loading. The warp knitted laminates were slightly stiffer than the woven laminates and both materials were comparably strong, Table I. In the weft direction the woven laminates were stiffer and stronger due to the reinforcing glass fibres present in the weft yarns. The transverse tensile failures of the warp knitted laminates resembled those of a pure thermoplastic with an extensive plastic deformation while the woven laminates were almost fully elastic until failure in both the warp and weft directions. Extensive delaminations and fibre pull-out took place during failure.

The experimental values of the tensile properties were slightly lower than those predicted by the rule of mixtures [7]. These deviations were probably caused by the poor fibre/matrix adhesion and the fibre misalignment during stacking and manufacturing. The modulus of the woven laminates in the warp direction was lower than that of the warp knitted due to the smaller fraction of glass fibres in this direction and also due to the crimp in the fibre architecture.

The in-plane shear modulus for the two materials were similar and the woven laminates had a marginally greater in-plane shear strength (calculated at the maximum load) than the warp knitted laminates, Table I. The shear failures of both materials were similar and involved large amounts of stress whitening. The scatter in the shear properties was larger for the warp knitted laminates and the fibre misalignment was believed to be responsible for this.

Flexure

In the static flexural tests the warp knitted laminates were stronger and stiffer than the woven laminates in the warp direction while the woven laminates were stronger and stiffer when tested in the weft direction, Table II. This latter effect was again due to the reinforcing glass fibres in the weft yarns of the woven laminates. The values of the moduli were consistently and significantly higher in flexure than in tension. The flexural modulus is dependent not only upon the fibre properties, fibre angles and fibre volume fraction but also on the stacking sequence. In all cases failures initiated on the compression side close to, or under, the loading pin. Cracks and limited delaminations propagated from the initial damage until final rupture of the specimen. Cracks were also seen to propagate along adjacent weft bundles in the woven laminates. The damage on the tensile face occurred in the form of fractures within the glass fibre yarns and cracking of the matrix between the yarns. This can be seen in the micrographs of the damage developed on the tensile face of a warp knitted specimen, Fig. 3.

The warp knitted laminates withstood a higher load before failure but exhibited a larger drop in their load bearing capabilities when compared to the woven laminates. The tests were stopped manually after the load drop since the toughness of the materials prevented the specimens from fracturing before the specimens folded in between the supports of the three-point bending jig.

The cross-ply laminates were also tested in three-point bending. No differences in the fracture behaviour was seen when compared to the unidirectional laminates. The flexural modulus of the warp knitted laminates was lower than for the woven laminates which was contrary to what was expected. This could be explained by the fact that the warp knitted cross-ply laminates were slightly thicker due to compaction problems during the compression moulding of the different laminates. This meant that the span to thickness ratio for the specimens was only 12:1 and consequently a significant amount of shear loading was present. Some few interlaminar cracks were seen during the tests. The values for the warp knitted cross-ply laminates in Table II are therefore not representative for pure flexure of the material.

Fibre fracture on the tensile face was the anticipated mode of failure for all the flexural tests and initially it was believed that the failures occurred due to a combination of tension and shear even though a span to thickness ratio of 16:1, as recommended in the ASTM standard, was used. However, the majority of the results available in the literature [13,14] do describe flexural failures initiating in the matrix on the compression face even at span to thickness ratios higher than 16:1. Static three-point bending tests of woven specimens utilising a span to thickness ratio of 32:1 were carried out in conjunction with the fatigue tests and these failures also initiated in compression. No difference in strengths or moduli was observed between the two different span to thickness ratios. The direct strain on the tensile face, as measured by means of strain gauges, was 1.2% at the initiation of the compression damage. Hence it was believed that the compression strength of the matrix limited the flexural performance of the laminates. Together with the previously discussed observations available in literature this implies that this might be the general case for many commingled thermoplastic matrix laminates, not only for this particular matrix polymer system.

The material used in the present work exhibited a poor fibre/matrix adhesion which might partly explain the mechanical properties that were lower than expected. The manufacturing process parameters for the material have not yet been optimised. Observations of a good quality fibre/matrix bond in commingled GF/PET composites were made by Ye and Friedrich [11] and Shonaike *et al.* [12]. One way to improve the adhesion between the reinforcing fibres and the matrix is by plasma treatment. Jang and Kim [15] improved the flexural strength and the interlaminar shear strength of co-woven CF/PEEK by 52% and 16% respectively by treating the fabric for 3min with a low temperature oxygen plasma treatment prior to compression moulding.

Fracture

There was no visible difference between the Mode I fracture behaviour of the woven and the warp knitted laminates. Unstable slip-stick crack growth occurred in about half of the specimens. Non-linearities were recorded in the load/displacement curve before the maximum load was reached. During testing a large amount of fibre pull-out was seen and this was responsible for the resistance curve effect in the fracture toughness and the unstable crack growth. In the woven laminates the crack followed the undulation of the warp yarns as the cracks propagated from the end of the non-adhesive insert, Fig. 4.

The initiation values of fracture toughness were calculated at the point where the load/deflection curve deviated from linearity as shown schematically in Fig. 5. The propagation values of fracture toughness were calculated from the conditions of steady state crack growth. No significant difference was detected between the toughnesses of the annealed woven laminate and those of the ordinary woven laminate. The fracture toughness of the warp knitted laminates was lower than for the woven laminates and this was due to the weft yarns in the woven laminates which made interlaminar crack propagation more difficult. The scatter in the fracture toughness data was greater for the mixed mode fractures in the cases of all three materials.

The fractographic examination of the Mode I fracture specimens revealed that the most dominant surface characteristic was fibre pull-out. Fig. 6 shows a large amount of fibre pull-out that occurred just ahead of the non-adhesive insert in a warp knitted specimen. Some of the pulled out fibres can be seen to extend back into the insert area and this most likely contributed to the relatively high values of crack initiation energies. The amount of fibre pull-out was larger on the fracture surface of the warp knitted specimens and the pull-out mainly occurred in bundles. In the woven laminates, on the other hand, the weft yarns limited the pull-out of fibres and yarns in the warp direction. The fibre pull-out was promoted by the poor strength of the fibre/matrix interface and the misalignment of the reinforcing fibres.

Crack propagation in the Mode II tests was more stable than in the Mode I tests. Fig. 7 shows a photograph of a warp knitted Mode II fracture specimen. To the left is the area of the non-

adhesive insert. The crack propagated from the end of the insert in a Mode II manner. The Mode II fracture surface is resin dominated with little fibre pull-out; this is the reason for the relatively smooth and light fracture surface in this region. The crack front is curved and this curvature is due to differing stress states across the width of the specimen with plane stress conditions being present at the edges and plane strain in the centre [16]. The right part of the specimen, which is where the specimen was broken up manually, shows the appearance of a Mode I dominated fracture with fibre pull-out being present in the form of both bundles and yarns.

In brittle thermoset matrix composites, cusps are the main Mode II fracture surface characteristic. Cusp formation in thermoplastic matrix composites has been seldom observed due to the inherent ductility of most thermoplastic polymer matrices. Ye and Friedrich [11] have reported the formation of slanted cracks on the edge of commingled GF/PET specimens during Mode II testing. In the present work, for both the woven and warp knitted laminates, a relatively many cusps were observed on the Mode II fracture surfaces, Fig. 8. The formation of cusps has been attributed to a brittle failure of the matrix [17-21] and can be described as the coalescence of brittle microcracks which form perpendicular to the resolved principal stresses just ahead of the crack tip, as shown schematically in Fig. 9. The angle of the cusps theoretically vary with the mixed mode loading ratio, from 0° for pure Mode I to 45° for pure Mode II.

The presence of cusps indicates that this PET matrix failed in a brittle manner; this was also supported by the appearance of the matrix failure in Mode I, Fig. 10. Shear deformation of the matrix was also seen in Mode II dominated fractures, Fig. 11, but this was not as extensive as in previous work on other semi-crystalline thermoplastic matrix composites, such as carbon fibre/poly ether ether ketone (CF/PEEK) [23,24].

Due to the relatively thick non-adhesive inserts used (i.e. 50μm), matrix pockets were seen at the end of the inserts and these might also have increased the initiation fracture toughness of the laminates.

Difficulties were encountered when using the MMB jig for the mixed mode fracture tests on these relatively highly compliant material systems. Large deflections were present due to the tough matrix and the relatively low modulus glass fibres. This resulted in the loading lever contacting either the end of the specimen or the base of the jig although it did not affect the measurement of initiation and propagation values of fracture toughness. The jig has since been modified to handle such large deflections. Stable mixed mode crack growth was seen in most cases for both the warp knitted and woven laminates. Figs. 12 and 13 show the experimentally determined failure loci for the three different materials in initiation and propagation.

The mixed mode 4:1 fracture surfaces had an appearance similar to the Mode I fracture surfaces displaying both fibre pull-out and brittle, featureless matrix failure. Fig. 14 shows the area around the insert in a woven specimen tested at mixed mode 1:1. In the micrograph it is seen that the insert in this particular laminate ended in a weft bundle (running from left to right in the micrograph) which may have affected the crack initiation in this particular sample. The matrix is featureless and there are fibre imprints and some pulled-out fibres. The end of the non-adhesive insert is seen to be wavy due to the underlying glass fibre warp yarns.

Cusps were also found in the Mode II dominated mixed modes, Fig. 15. However, the amount of cusps was smaller than for pure Mode II. Compared to brittle epoxy matrix composites, cusps in the GF/PET material system were very rare and not as well defined, i.e. the cusps varied in size and appearance (compare Figs. 8 and 15). The cusps in the different fracture modes also stood more upright (i.e. the cups angle was larger) than the cusps previously observed in epoxy matrices [21,25].

Fatigue

The fatigue performance of composite component is important in applications where the material is subjected to cyclic loadings or deformations. In the presence of macroscopic defects or stress concentrations cracks will initiate and grow. Macroscopically the crack growth can often be described by a power-law type relationship. However, this crack growth will be very complex when, for example, textile reinforcements are used as was observed by Hoffman and Wang [26] in chopped E-glass composites where the glass fibres were knitted together with continuous PET yarns. The notched specimens where loaded in tension and the typical fatigue crack propagation was characterised by acceleration, retardation and deceleration caused by the development of damage zones in the complex composite microstructure. The authors concluded that the knitting PET fibres contributed to the crack growth resistance by the introduction of elaborate failure mechanisms.

Information on the fatigue performance of continuous fibre reinforced engineering thermoplastics is very scarce in literature. Gauthier *et al.* [27] examined the interlaminar fracture and fatigue performance of unidirectional GF/PET compression moulded at different temperatures (270°C and 300°C) and with different cooling rates (8°C/min and 60°C/min). A brittle behaviour was observed for the slowly cooled specimens while the rapidly cooled specimens exhibited more ductile failures. The optimum toughness was obtained for low moulding temperatures and high cooling rates. The fatigue behaviour was assessed using a criterion of a 10% decrease in flexural modulus and a typical S/N-curve can be seen in Fig. 16. The authors also reported that for the specimens that had been moulded at the higher temperature, i.e. 300°C, the improved wetting and interface strength limited the fatigue behaviour and energy dissipation. Fig. 17 shows the fatigue response of unidirectional continuous fibres and discontinuous fibres Kevlar 49/J-2 (J-2 is an amorphous polyamide copolymer) composites as determined by Okine *et al.* [28]. The discontinuous fibre composites (fibre lengths of 25-150mm

and an orientation with 85% of the fibres within the ±5° directions) behaved in a similar manner as the continuous fibre composites.

In the present work some problems were initially encountered during the fatigue testing. The specimens did in some cases slide sideways and loose their alignment in the three point bending jig. This was believed to be due to the fibre misalignment in the laminates. The rig was later modified with shallow grooves preventing the sliding of the specimens.

The obtained fatigue results are shown in Fig. 18. As expected the failure load decreases as the number of load cycles increase. At all load levels the modes and mechanisms of fatigue failures were the same as for static failures. The damage initiated on the compression side, usually a small distance away from the loading pin and also close to the weft bundles, Fig. 19 and Fig. 20. The damage was seen as lines of stress whitening which was the result of matrix cracking and crazing. At an increased load or at a higher number of load cycles the damage progressed out from the loading area as seen schematically in Fig. 21. This damage was in the static tests accompanied by a small load drop. As the tests continued the damage finally propagated through the thickness and failure on the tensile side occurred. Tensile matrix cracking, typically as shown in Fig. 22, accumulated in the developing damage zone during the tests. The specimens were generally still able to carry a significant load after the tensile failure even though a few specimens fractured catastrophically with visible fibre fractures across the full width of the tensile face. This variability in failure behaviour is not desirable from a design point of view and this issue needs to be addresses further.

By improving the adhesion between the fibres and the matrix the fatigue life ought to increase as crack propagation along the interface would be more difficult. Friedrich [29] reported an improved fatigue life of injection moulded GF/PET with a higher fibre/matrix interface quality. In this work Friedrich also observed that the fatigue crack growth rate was higher in areas with highly aligned fibres.

During the SEM examination of the fracture surfaces a few unusual features were seen. Fig. 23 shows a wavy matrix pattern close the final failure. These patters were occasionally seen in some of the specimens at different load levels and the formation of these are not fully understood. One explanation may be local plastic deformation of the matrix under the cyclic compression loading. During previous fractographic work on statically failed specimens of the same material this phenomenon was not observed. Fibrils bridging fairly large matrix cracks were also observed, Fig. 24 and this was somewhat surprising in view of the evidence of a fairly brittle matrix failure discussed earlier.

Conclusions

The traditional textile processes, such as weaving and warp knitting, enable a rapid production of reinforcement for structural composites. In the present work the response to mechanical loads of novel commingled warp knitted and woven glass fibre reinforced polyethylene terephthalate (GF/PET) laminates has been characterised. The mechanical properties of the two materials were determined under tension, in-plane shear and flexure. The warp knitted material was marginally stiffer and stronger when compared to the woven material. Some manufacturing problems regarding, e.g. accurate fibre alignment, fibre/matrix interface quality and variability in mechanical properties, still persist.

The flexural fatigue properties were determined for the woven laminates by means of three point bending tests with a loading ratio of R=0.1 at stress levels of 50-90% of the ultimate static strength. The laminates exhibited a decreasing failure load with an increasing number of load cycles. The decrease was similar to those previously reported in literature for continuous fibre reinforced thermoplastic materials with a maximum load reduction of about 40% for 10^6 load cycles. The failures generally initiated on the compression face and a damage zone developed. An SEM examination of the specimens identified some of the mechanisms involved in failure to be

tensile matrix failure, crazing, formation of wavy surface matrix features and tensile and compression glass fibre breakage.

The Mode I, Mode II and mixed mode (Mode I:II ratios 4:1, 1:1 and 1:4) interlaminar fracture toughnesses of the laminates were determined by means of the double cantilever beam (DCB) and mixed mode bending (MMB) tests respectively. The initiation fracture toughnesses for the woven materials were around 1.1kJ/m^2 and in Mode II around 1.2kJ/m^2 for Mode I and Mode II respectively. For the warp knitted material the corresponding values were 0.9kJ/m^2 and 1.3kJ/m^2. The propagation toughnesses were 2-3 times higher for all materials tested.

The main fractographic features, as determined by an scanning electron microscopy (SEM) examination, of the Mode I dominated failures were a brittle matrix failure and large amounts of fibre pull-out. As the Mode II loading component increased, the amount of fibre pull-out was reduced and the features of the matrix appeared to be more sheared. Cusps were found on the fracture surfaces of specimens tested in pure Mode II and mixed mode I:II=1:4. Cusps are normally not found in thermoplastic matrix composites.

Both materials offer a good combination of mechanical properties and a toughness and are promising for structural applications in, for example, the transportation industry.

References

1 A.G. GIBSON and J-A. MÅNSON, *Composites Manufacturing* **3** (1992) 223.
2 L. YE and K. FRIEDRICH, *Journal of Materials Science* **28** (1993) 773.
3 A. RAMASAMY and Y. WANG, *Polymer Composites* **17** (1996) 515.
4 J.W.S. HEARLE and G.W. DU, *Journal of the Textile Institute* **81** (1990) 360.
5 A.B. STRONG, in "High performance and engineering thermoplastic composites" (Technomic Publishing Company, Pennsylvania, USA, 1993).
6 N. SVENSSON, R. SHISHOO and M. GILCHRIST, "Manufacturing of thermoplastic composites from commingled yarns - A review", accepted for publication in *Journal of Thermoplastic Composite Materials* (1997).
7 N. SVENSSON, R. SHISHOO and M. GILCHRIST, "Fabrication and Mechanical Response of Commingled GF/PET Composites", accepted for publication in *Polymer Composites* (1997).
8 J.H. CREWS and J.R. REEDER, *NASA TM100662* (1988)
9 J.R. REEDER and J.H. CREWS, *NASA TM102777* (1991).
10 A.J. KINLOCH, Y. WANG, J.G. WILLIAMS and P. YAYLA, *Composites Science and Technology* **47** (1993) 225.
11 L. YE and K. FRIEDRICH, *Composites* **24** (1993) 557.
12 G.O. SHONAIKE, M. MATSUDA, H. HAMADA, Z. MAEKAWA and T. MATSUO, *Composite Interfaces* **2** (1994) 157.
13 H. HAMADA, Z.-I. MAEKAWA, N. IKEGAWA, T. MATSUO and M. YAMANE, *Polymer Composites* **14** (1993) 308.
14 N.S. CHOI, H. YAMAGUCHI and K. TAKAHASHI, *Journal of Composite Materials* **30** (1996) 760.
15 J. JANG and H. KIM, *Polymer Composites* **18** (1997) 125.
16 W. BRADLEY, C. CORLETO and M. HENRIKSEN, M., in Proceedings of Sixth International Conference on Composite Materials (ICCM-VI) London, edited by F.L. Matthews, N.C.R. Buskell, J.M. Hodgkinson, and J. Morton (Elsevier Applied Science Publishers, 1987) p. 3378.
17 T. JOHANNESSON and M. BLIKSTAD, in ASTM STP 876 (American Society for Testing and Materials, 1985) p. 411.
18 T. JOHANNESSON, P. SJÖBLOM and R. SELDÉN, *Journal of Materials Science* **19** (1984) 1171.
19 L. ARCAN, M. ARCAN and I.M. DANIEL, in ASTM STP 948, (American Society for Testing and Materials, 1987) p. 41.
20 M.L. BENZEGGAGH and M. KENANE, *Composites Science and Technology* **56** (1996) 439.
21 N. SVENSSON and M. GILCHRIST, "Mixed Mode Delamination of Multidirectional Carbon Fibre/Epoxy Laminates", submitted to *Mechanics of Composite Structures* (1997).
22 M.R. PIGGOT, *Composite Science and Technology* **55** (1995) 269.
23 S.L. DONALDSON, *Composites* **16** (1985) 103.
24 A. BEEHAG and L. YE, *Composites Part A* **27A** (1996) 175.
25 M.D. GILCHRIST and N. SVENSSON, *Composites Science and Technology* **55** (1995) 195.
26 L. HOFFMANN and S.S. WANG, *Engineering Fracture Mechanics* **52** (1995) 1151.
27 M. GAUTHIER, J. CHAUCHARD, B. CHABERT and J.P. TROTIGNON, *Die Angewandte Makromolekulare Chemie* **221** (1994) 137.
28 R.K. OKINE, D.H.EDISON and N.K. LITTLE, *Journal of Reinforced Plastics and Composites* **8** (1990) 70.
29 K. FRIEDRICH, *Plastics and Rubber Processing and Applications* **3** (1983) 255.

TABLES

TABLE I The mechanical properties of the two different GF/PET laminates [7].

Mechanical property	Woven	Warp knitted
Tensile modulus, warp (GPa)	22.9	28.2
Tensile strength, warp (MPa)	510.4	486.6
Tensile modulus, weft (GPa)	6.9	3.5
Tensile strength, weft (MPa)	130.9	6.6
In-plane shear modulus (GPa)	4.4	4.3

TABLE II The flexural properties of the unidirectional and warp knitted laminates [7].

	Woven	Warp knitted
Flexural modulus, warp (GPa)	29.0	35.0
Flexural strength, warp (MPa)	493.6	747.2
Flexural modulus, weft (GPa)	10.7	4.6
Flexural strength, weft (MPa)	214.0	24.7
Flexural modulus, cross-ply (GPa)	21.2	17.4
Flexural strength, cross-ply (MPa)	318.8	323.4

FIGURE CAPTIONS

Figure 1 The two commingled yarn fabrics used for the fabrication of laminates. To the left is the woven fabric, in the middle the warp knitted fabric and to the right an optical micrograph of the PET binding yarn which holds the warp yarn together in the warp knitted fabric.

Figure 2 Clean fibres on the fracture surface of a mixed mode 1:1 woven sample showing the poor adhesion between the fibres and the matrix (i.e. clean fibres). The induced global crack propagation direction is from the bottom to the top in the micrograph. Tilt angle 30°.

Figure 3 The tensile failure of a warp knitted three point bending specimen. The glass fibre yarns hold together during the fracture. Cracks in the matrix are seen (to the right) between the glass fibre bundles.

Figure 4 Fibre bridging during a Mode I test. The crack front is seen to be slightly bent out of plane and crack propagation followed the undulated paths of the warp yarns.

Figure 5 The schematic load/displacement curve of a DCB test. The fracture toughness initiation values were calculated from the conditions at the onset of non-linearity.

Figure 6 Extensive fibre pull-out ahead of the Nylon 6 insert of a warp knitted Mode I specimen. Some of the pulled out fibres extended back into the insert area. The induced global crack propagation direction is from the bottom to the top in the micrograph. Tilt angle 10°.

Figure 7 A photograph of a backlit warp knitted Mode II specimen. To the left is the end of the insert. The crack has propagated in Mode II which has a bright matrix dominated appearance. The crack front is curved (shown by the dashed line). To the right is the area where the sample has been broken up manually by hand, i.e. crack propagation in a Mode I dominated manner.

Figure 8 Rows of cusps evident between fibres on a Mode II fracture surface of a woven laminate. The induced global crack propagation direction is from the bottom to the top in the micrograph. Tilt angle 30°.

Figure 9 The formation of cusps as the coalescence of brittle micro cracks ahead of the crack tip (after Piggot [22]).

Figure 10 Tensile brittle matrix failure of a Mode I fracture surface of a warp knitted specimen. The induced global crack propagation direction is from the bottom to the top in the micrograph. Tilt angle 0°.

Figure 11 Matrix shear deformation on the surface of a woven Mode II fracture specimen. The induced global crack propagation direction is from the bottom to the top in the micrograph. Tilt angle 30°.

Figure 12 The experimentally determined fracture toughness initiation values for the three different materials.

Figure 13 The experimentally determined fracture toughness initiation values for the three different materials.

Figure 14 The area around the insert of an annealed woven specimen at low magnification. The crack has propagated in mixed mode 1:1. A slight waviness of the insert is seen as well as a large resin pocket (upper right corner). The induced global crack propagation direction is from the bottom to the top in the micrograph. Tilt angle 30°.

Figure 15 Small cusps with the tip bent over in the global crack propagation direction as seen on a mixed mode 1:4 fracture surface in an annealed woven specimen. The induced global crack propagation direction is from the bottom to the top in the micrograph. Tilt angle 30°.

Figure 16 The Wöhler curve for two unidirectional GF/PET laminates processed at 270°C and 300°C respectively (after Gauthier *et al.* [27]).

Figure 17 The tension-tension fatigue behaviour of unidirectional continuous fibres and ordered staple fibres Kevlar49/J-2 laminates (J-2 is a polyamide copolymer) (after Okine *et al.* [28]).

Figure 18 The S-N curve obtained for the woven material. The general trend is a gradual decrease of failure load with increasing number of load cycles. The scatter is fairly large, especially at higher load levels.

Figure 19 A schematic picture of the compression face of a flexural fatigue specimen. The failure initiated on the tensile face as compression damage just outside the loading pin, often at adjacent weft yarns. Damage then accumulated and propagated through to the tensile face and final failure occurred.

Figure 20 The compressive damage away from the loading pin on a flexural fatigue specimen. The longitudinal direction of the specimen if from the bottom to the top in the micrograph.

Figure 21 Close up of a compressive fibre bundle failure. The glass fibres shows evidence of buckling due to the compressive loads. The longitudinal direction of the specimen if from the bottom to the top in the micrograph.

Figure 22 Cracking of the matrix, as seen in the micrograph, was one of the mechanisms that accumulated during the fatigue test. The longitudinal direction of the specimen if from the bottom to the top in the micrograph.

Figure 23 A wavy surface pattern was occasionally seen in the failure area on the fatigue specimens. The mechanisms for the formation of these are not fully understood.

Figure 24 Fibrils bridging a matrix crack close to the location of the primary compressive damage.

FIGURES

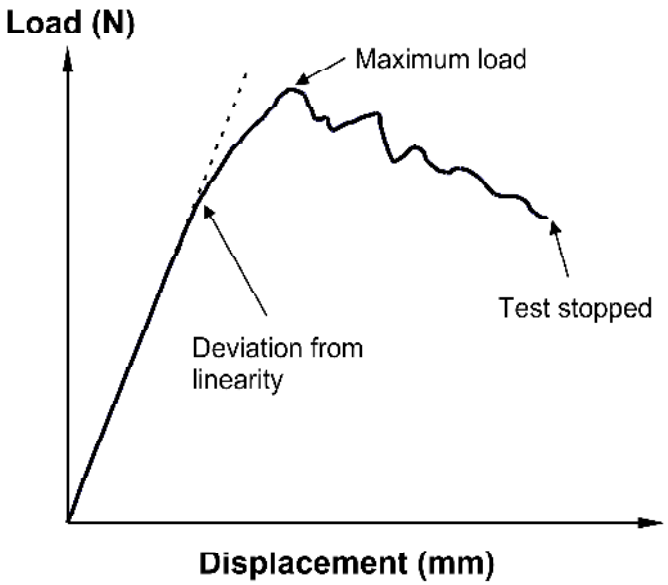

Figure 5

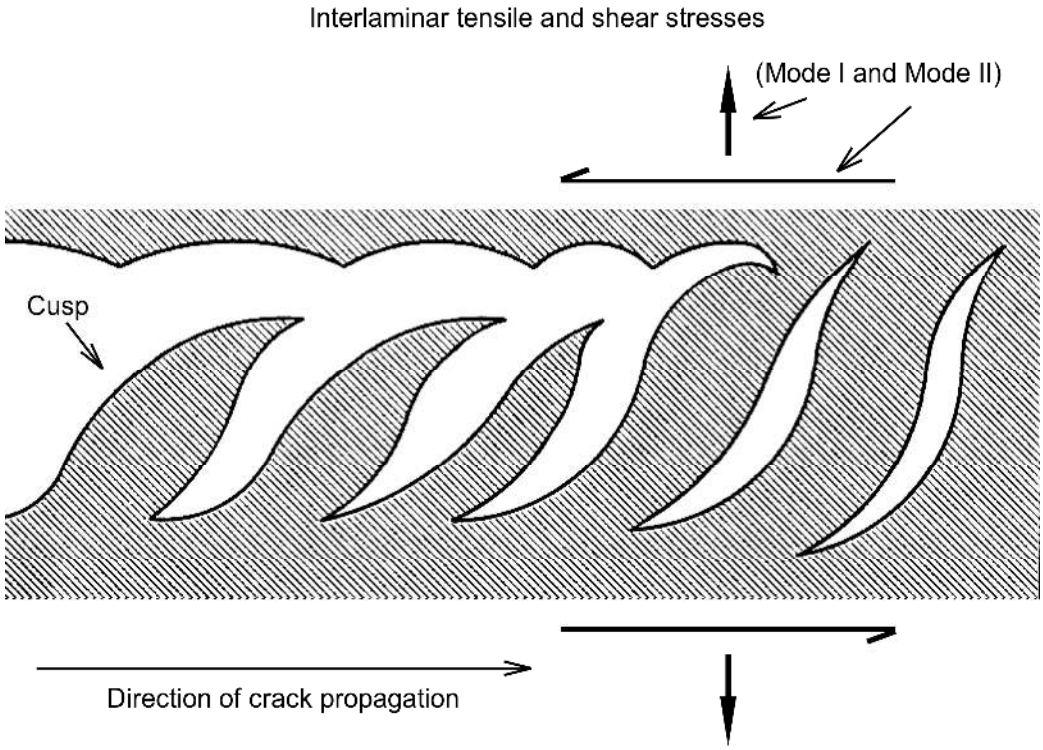
Interlaminar tensile and shear stresses
(Mode I and Mode II)
Cusp
Direction of crack propagation

Figure 9

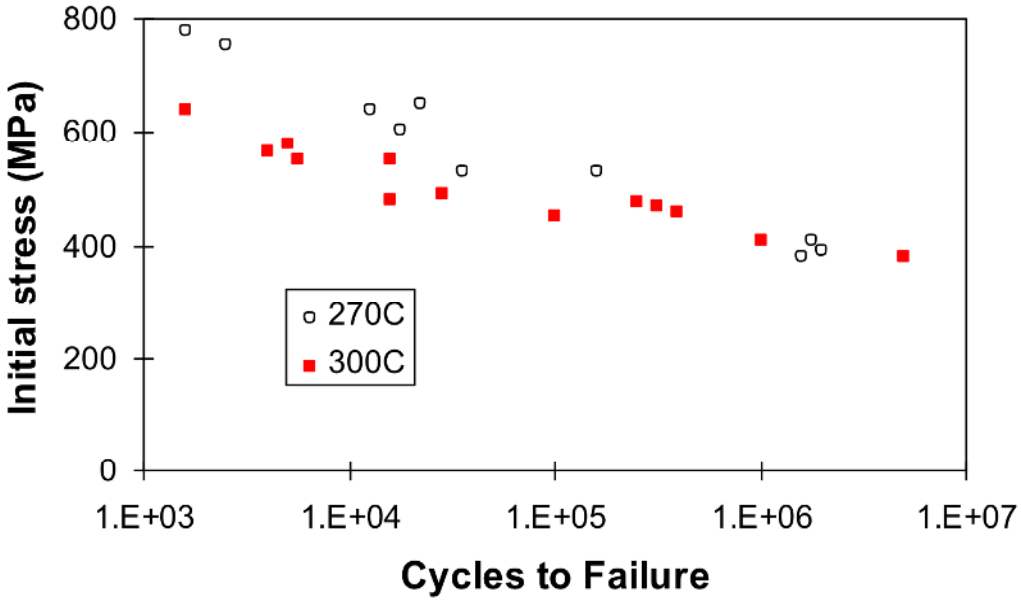
800
600
400
200
0
Initial stress (MPa)
270C
300C
1.E+03
1.E+04
1.E+05
1.E+06
1.E+07
Cycles to Failure

Figure 16

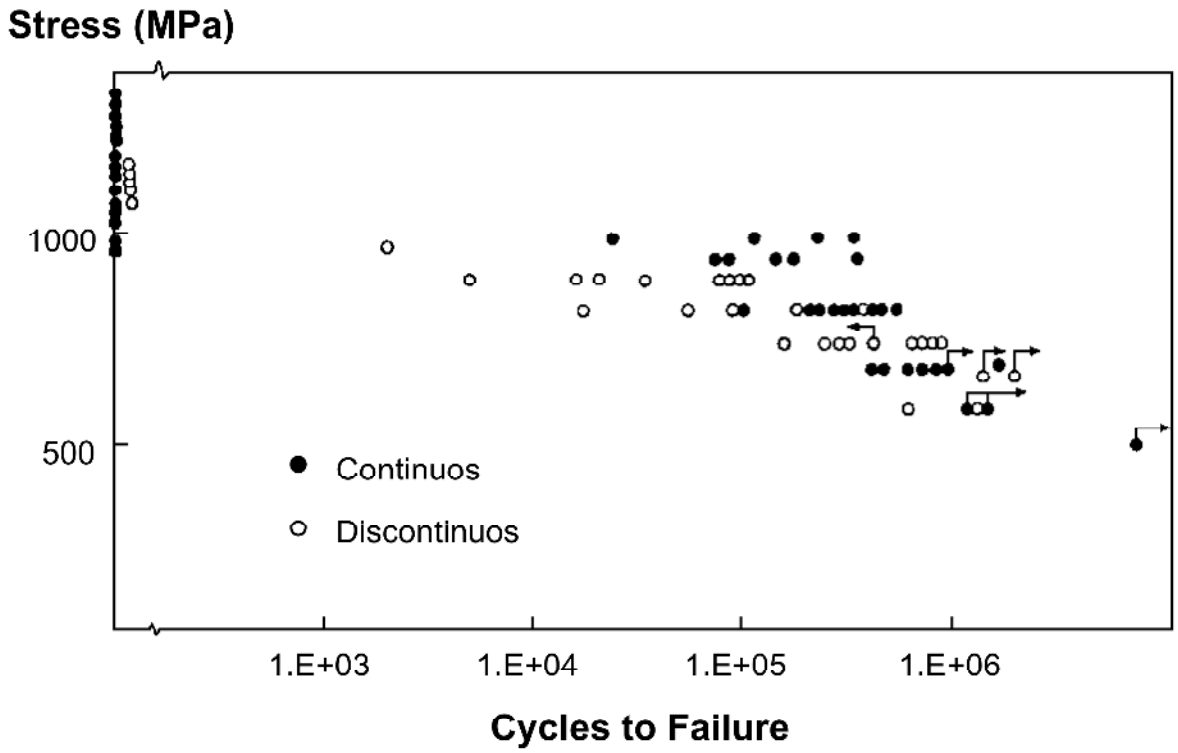
Stress (MPa)
1000
500
Continuos
Discontinuos
1.E+03
1.E+04
1.E+05
1.E+06
Cycles to Failure

Figure 17

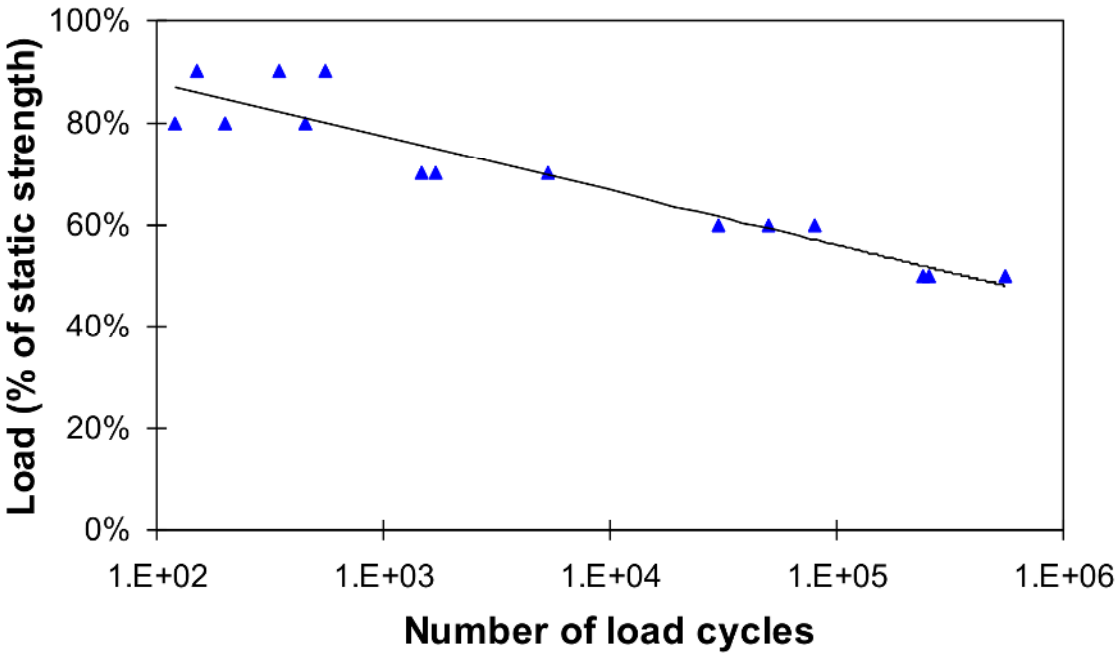
Load (% of static strength)
100%
80%
60%
40%
20%
0%
1.E+02
1.E+03
1.E+04
1.E+05
1.E+06
Number of load cycles

Figure 18

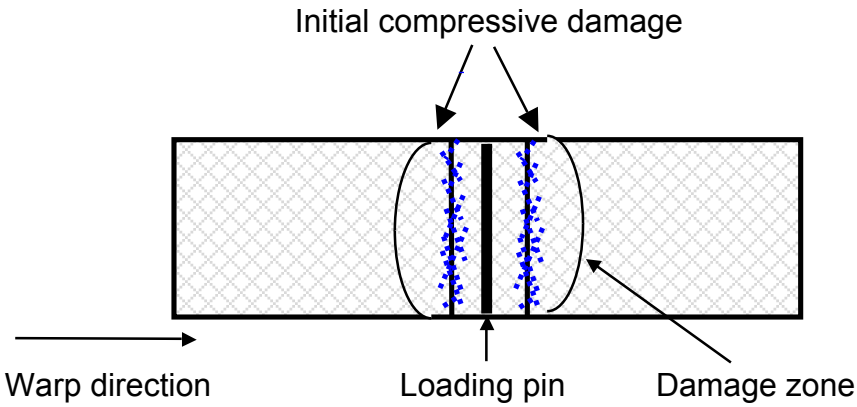
Initial compressive damage
Warp direction
Loading pin
Damage zone

Figure 21